FLUME MEASUREMENTS OF SEDIMENT ERODIBILITY IN BOSTON HARBOR

By Thomas M. Ravens[1] and Philip M. Gschwend[2]

ABSTRACT: To obtain in situ measurements of sediment erodibility in defined bottom shear stress environments, a portable, straight flume was built, tested, and deployed in the field for six experiments at three locations in Quincy Bay of Boston Harbor, Mass. The flume had a 1.0-m-long inlet section, which included a boundary-layer trip and a roughened, plexiglass bottom; this design prevented erosion of the sediment bed in the boundary-layer-development region. Downstream of the inlet section was a 1.2-m-long sediment test section, which had a laboratory-verified, uniform bottom stress. In the absence of algal mats, our flume experiments on sites exhibiting a range of bed properties indicated quite uniform erodibility, with a critical shear stress τ_c of 0.10 $\pm$ 0.04 Pa and an erosion rate constant M of 3.2 $\pm$ 0.2 $\times$ 10^{-3} kg m^{-2} s^{-1} Pa^{-1} (R^2 = 0.92, N = 17, where N is the total number of erosion rate measurements made in the absence of algal mats). The measured rates were consistent with those of many other in situ studies. We observed markedly reduced erodibility in early October 1995 when the sediment was covered by a benthic diatom mat, and measured erosion rates were lessened by 50–80%. The possibility of depth-dependent sediment erodibility in near surface (top 3 mm) was investigated by calculating a set of depth-dependent erosion parameters. The parameters obtained suggested that both the critical shear stress and the erosion rate constant were depth-sensitive (both doubling by 1 mm into the sediment).

INTRODUCTION

Knowledge of the erosion properties of cohesive sediment beds is essential for sediment resuspension and transport modeling. Furthermore, because the cohesive sediment in many urban estuaries is contaminated, sediment erosion and resuspension may affect the health of the local ecosystem. Unfortunately, the erosion properties cannot be reliably predicted from environmental parameters (e.g., grain size, water content, or organic content), and direct measurement of erodibility is necessary (McCave 1984). One way to obtain knowledge of sediment erodibility is to use a flume to apply a known bottom shear stress on the sediment bed, to observe the rate of erosion, and to infer the erosion parameters given some model of the erosion process (Krone 1976; Maa et al. 1993; McNeil et al. 1996). Alternatively, the erosion/resuspension due to natural processes (e.g., tides or wind waves) can be observed and the erosion properties inferred (Lavelle et al. 1984; Luettich et al. 1990; Sanford et al. 1991).

Often, a flume is employed because nature cannot be relied upon to provide the conditions of interest at a given time. Also, use of a flume allows the assessment of different sites and yields data on erosion processes without having to consider other complicating sediment transport processes that would be present under natural conditions. Historically, laboratory flumes have been employed for the most part. Sediment samples are collected from the field and redeposited in the laboratory flume (Young 1975; Krone 1976). Alternatively, sediment cores are taken and placed ''undisturbed'' at the flume bottom (Rhoads et al. 1978; McNeil et al. 1996). The work of Young (1975), who deployed an in situ flume as well as a laboratory flume, suggests that the laboratory flume can overestimate the critical shear stress by a factor of 2. However, if naturally occurring infauna, which churn up the sediment and make it more erodible, are allowed to populate the sediment in the laboratory flume, the difference between the laboratory and in situ critical shear stresses can be narrowed. Other workers have shown that the presence of benthic organisms that secrete adhesive chemicals can decrease the bed erodibility (Holland et al. 1974; Daborn et al. 1993). The difficulty of maintaining a healthy and representative benthic community in the laboratory makes an in situ flume more attractive.

Flume geometry is also an important issue. Annular flumes have the advantage that they achieve a fairly uniform shear stress environment, although they are subject to secondary flows (Maa 1993). Straight flumes, in contrast, are characterized by nonuniform flow in the inlet section where the boundary layer is developing (Gust and Morris 1989). However, if the boundary layer is ''tripped'' or stimulated, the distance over which the boundary layer develops can be significantly reduced. Furthermore, the conventional, straight flume design can be improved by limiting the sediment bed test section to those parts of the flume where developed, uniform flow has been established (Butman and Chapman 1989).

In this study, a straight flume was constructed and applied in situ so that testing of sediment beds in Boston Harbor could be done while minimizing disturbances. Visual inspection of the undisturbed sediment revealed that it was easily eroded, suggesting that it may be difficult to bring sediment to the laboratory without substantially altering it. Furthermore, sediment cores revealed the presence of benthic organisms whose influence on sediment erodibility might be difficult to reproduce in the laboratory. A straight flume was chosen because it is simple and inexpensive to build and deploy and because some of its apparent disadvantages (e.g., flow nonuniformity) could be avoided with design modifications.

It should be noted that in Quincy Bay, sediment erosion is largely wave-induced. Therefore, we are presuming that measurements of erodibility under steady flow conditions are also applicable to unsteady flows.

METHODS

Flume Design

The flume was constructed with 1-cm-thick acrylic plastic (plexiglass). Plexiglass is easy to cut and connect, allows for visual inspection of the erosion processes taking place within the flume, and enables nonintrusive laser Doppler anemometer measurements of velocity within the flume. The flume was 2.4 m long with a width and height of 12 and 6 cm, respectively (Fig. 1). The flume had a grill over the entrance to keep large (>1 cm) objects out. A 2.5-cm-high lateral bar was attached to

[1]Postdoctoral Researcher, Dept. of Envir. Phys., EAWAG, Swiss Fed. Inst. for Envir. Sci. and Technol., CH-8600, Duebendorf, Switzerland.

[2]Prof., Ralph M. Parsons Lab., Dept. of Civ. and Envir. Engrg., 48-415, Massachusetts Inst. of Technol., Cambridge, MA 02139.

Note. Discussion open until March 1, 2000. To extend the closing date one month, a written request must be filed with the ASCE Manager of Journals. The manuscript for this paper was submitted for review and possible publication on January 11, 1999. This paper is part of the ***Journal of Hydraulic Engineering***, Vol. 125, No. 10, October, 1999. ©ASCE, ISSN 0733-9429/99/0010-0998–1005/$8.00 + $.50 per page. Paper No. 20010.

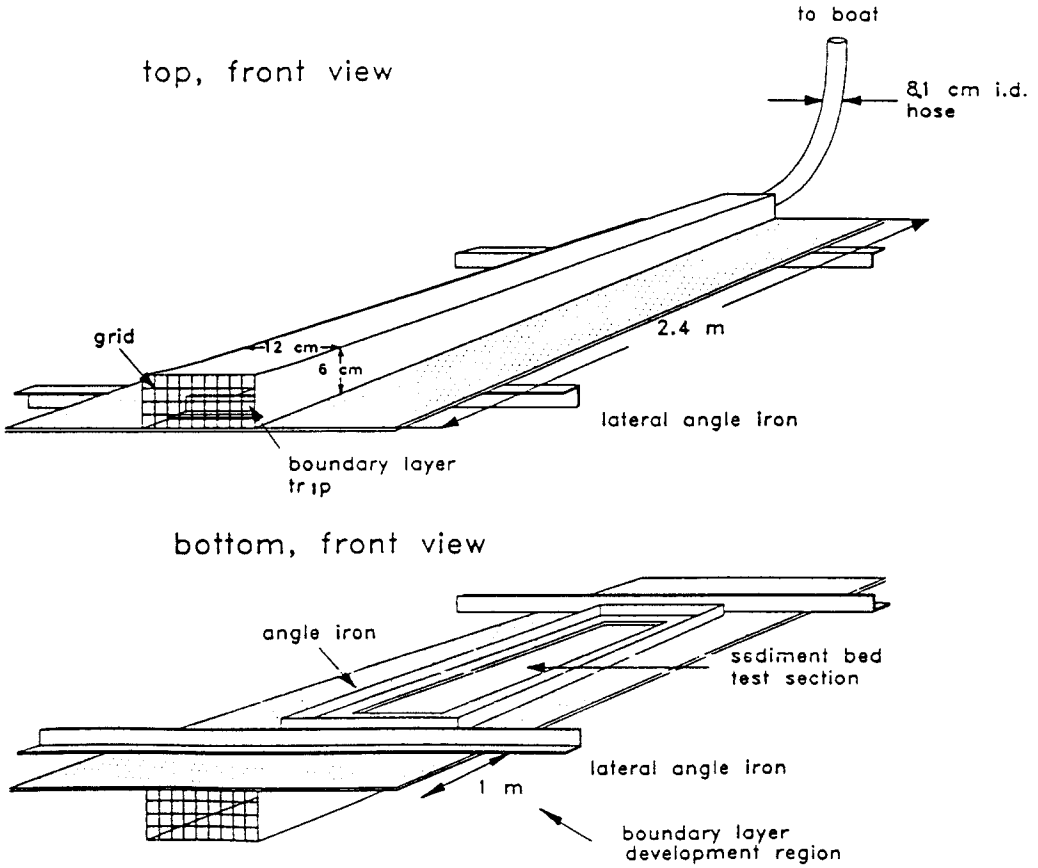

FIG. 1. Diagram of Flume

the floor of the flume just inside the entrance to stimulate development of the bottom boundary layer. The first 1 m of the inlet end of the flume was fitted with a thin plastic bottom, roughened with lacquered, 300-μm sand. The bottom prevented the developing flow from shearing the sediment bed. The next 1.2 m of the flume housed the erosion zone where the developed flow (see below) was allowed to shear the bed. The outlet section had a 27-cm-long floor that protected that portion of the bed from the turbulence and nonuniform flow associated with the exit. Running the length of the flume were two, 12-cm-wide plexiglass ''feet'' which prevented the flume from sinking into the mud. Longitudinal and lateral angle irons (4×4 cm) were attached around the flume's bottom opening forming a bottom edge that, during erosion experiments, was imbedded in the sediment preventing water from infiltrating from the sides. Additional lateral angle irons were attached to the flume bottom at the entrance and exit to help stabilize the flume during erosion experiments. Water was pulled through the flume by a shipboard 3.6 kW, gasoline-powered, Teele pump (Dayton Electric Manufacturing Co., Niles, Ill.) that was connected to the flume via a 12-m, 8.1-cm-internal diameter, thick walled, rubber hose. Flow in the flume was controlled with a ball valve downstream of the pump and occasionally by the pump throttle. A Signet flow meter (El Monte, Calif.) positioned between the pump and the ball valve indicated the flow rate through the system. Just downstream of the pump, a small portion of the flow was diverted through a Hach turbidimeter (Loveland, Colo.).

An important principle behind the flume operation was the relationship between the flow rate through the flume Q (L s^{-1}) and the shear stress τ (Pa) applied to the sediment bed. The connection was made on the basis of the Darcy-Weisbach friction factor f, which relates τ and the cross-sectional area-averaged velocity $U = Q$/area (m s^{-1})

$$\tau = \rho(f/8)U^2 \tag{1}$$

where ρ = water density (kg m^{-3}). The Moody diagram (Daily and Harleman 1966), modified for flow through a rectangular channel, provides the friction factor as a function of the relative roughness ($k_s/4R_h$) and the Reynolds number ($\mathrm{R} = 4R_hU/\nu$) where k_s is the median sediment grain size, R_h is the hydraulic radius (cross-sectional area/channel perimeter), and ν is the kinematic viscosity. The Moody diagram assumes that the walls are equally rough from a hydrodynamic point of view. The friction factor obtained with a typical sediment roughness of 100 μm and flow rate of 1.0 L s^{-1} ($f \sim 0.029$) was not significantly different from the friction factor obtained assuming smooth walls ($f \sim 0.027$). With the friction factor and measurements of Q, therefore, the average bottom shear stress can be obtained for a given flow rate. For a range of flow rates (Q = 1.0–3.5 L s^{-1}), the corresponding bottom shear stresses τ (Pa) were obtained, and a power law fit for our system was derived

$$\tau = 0.0566Q^{1.84} \tag{2}$$

Flume Testing

Two types of tests were performed to ensure that the flume was operating properly. First, depth profiles of velocity along the centerline of the flume were made as a function of flow rate. The bottom stress was then estimated from analysis of the logarithm of distance above the flume bottom versus velocity (Fig. 2). Velocity measurements were made with a laser Doppler velocity meter (Dantek, Denmark) on the basis of 30 s of data collected at 100 Hz. For flows of 1.1 L s^{-1} or greater, the logarithm z versus velocity profile was linear, and it did not vary within the test zone of the flume. These results indicated that the flow was fully developed in the erosion zone

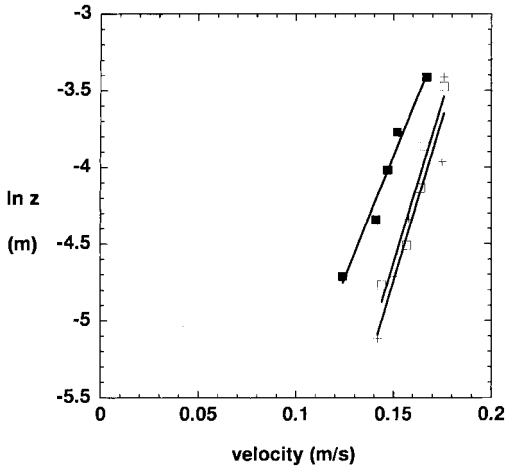

FIG. 2. Logarithm *z* (Height above Bottom) versus Measured Velocity at Flow Rate of 1.1 L s^{-1}. Velocity Was Measured at 0.6 m (■), 1.2 m (□), and 1.8 m (+) into Flume

of the flume with such flows. The results also validated the use of (2) for estimating bottom stress. For example, linear analysis of the profiles (at 1.1 L s^{-1}) indicated centerline bottom stresses of 0.076 ± 0.031 and 0.080 ± 0.023 Pa at 1.2 and 1.8 m into the flume, respectively. By comparison, (2) indicates a bottom stress of 0.067 Pa at this flow rate. The centerline stresses would be expected to be higher than the average as the flow and stress is greater in the center.

Second, a flume experiment was performed with sorted (mostly 70–180 μm) sand, for which the erosional behavior was estimated from the Shields diagram (Graf 1984). The test indicated initiation of motion at a bottom shear stress of about 0.1 Pa, which agrees with the expected critical stress for the fine fraction of the sand. Overall, the flume-generated shear flows were consistent with expectations based on theory.

Site Description

Quincy Bay is a shallow embayment located in outer Boston Harbor in the southwest corner of the gulf of Maine (Fig. 3). For decades contaminants were discharged into Quincy Bay from a combined sewer overflow at Moon Head and a wastewater treatment plant at Nut Island (Leo et al. 1993). Quincy Bay's sediment is contaminated with metals (Fitzgerald 1980; Gardner and Pruell 1988) and organic contaminants (Shiaris and Jambard-Sweet 1986; Gardner and Pruell 1988).

Three sites in Quincy Bay (FL1, FL2, and FL3; Fig. 3) were chosen for flume experiments. The three sites all had silty sediment and were relatively shallow (Table 1). Site FL2 was in deeper water and had finer, more organic sediment than the other two. These sites normally see little hydrodynamic forcing because tidal currents are fairly weak [<25 cm s^{-1} (Signell and Butman 1992)]. However, in the event of onshore storms, Quincy Bay is subject to in-harbor-generated wind waves as well as some ocean swell, which together can apply bottom skin friction stresses of 0.3 Pa or more (Ravens 1997).

Experimental Procedure

The experimental procedure was to first lower the flume to the sediment bed with the inlet facing the current. Scuba divers

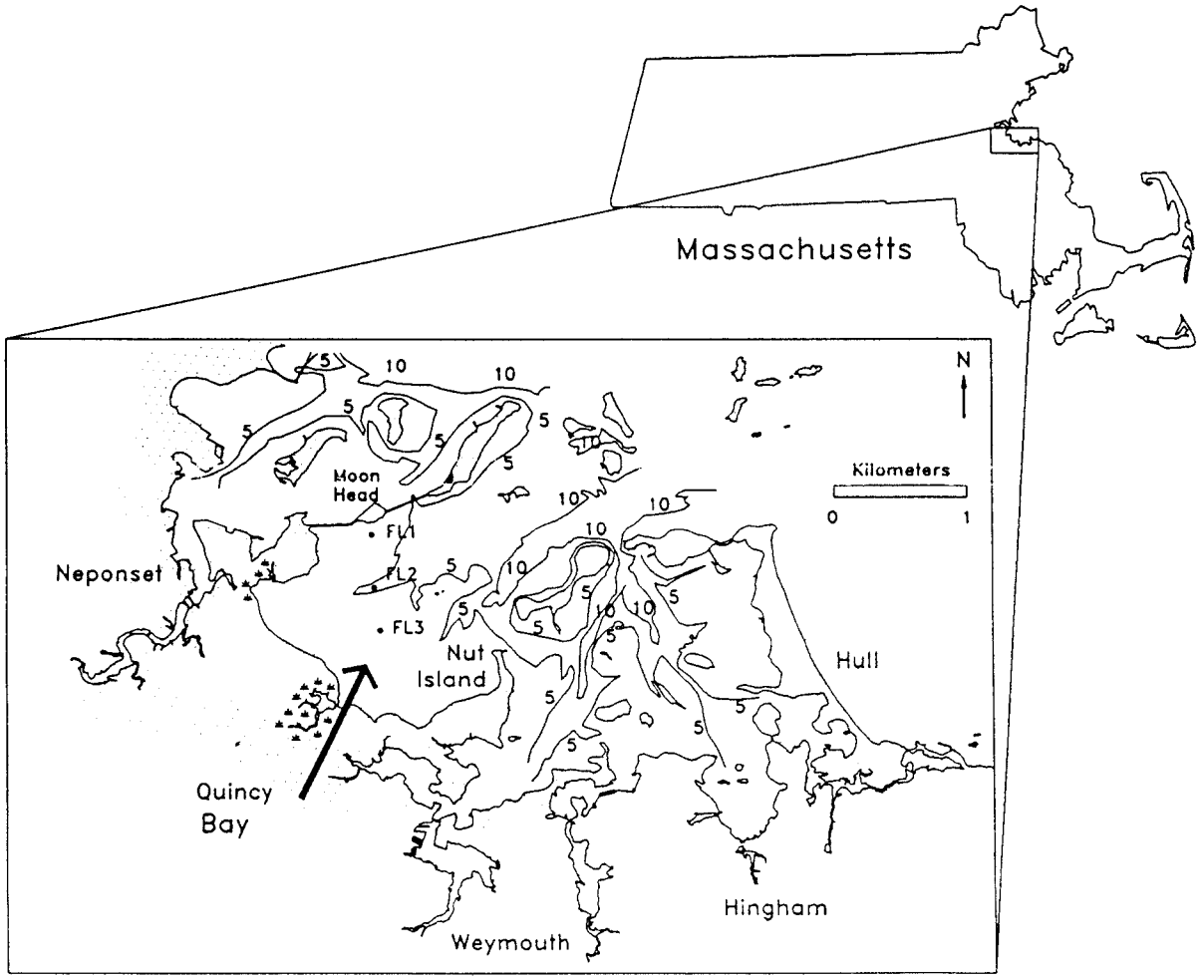

FIG. 3. Location of Flume Experiment Sites (FL1, FL2, and FL3) in Qunicy Bay in Outer Boston Harbor. Water Depth Contours Show Depth (m) at Middle Tide

TABLE 1. Characteristics of Sites at which Flume Experiments Were Conducted

Site (1)	Mean depth (m) (2)	Sediment[a] porosity (%) (3)	Sand[b] content (%) (4)	Silt[b] content (%) (5)	Clay[b] content (%) (6)	Average sediment size[b] D_{50} (μm) (7)	Sediment organic content (%) (8)
FL1	3.8	76	37	51	12	60	3.0[c]
FL2	6.1	82	11	62	27	30	4.5[c]
FL3	4.2	78	25	64	11	50	3.0[d]

[a]Estimated on basis of sediment drying (24 h, 60°C) assuming a solid density of 2.5 g/cm^3.
[b]M. Bothner (personal communication, 1994).
[c]Organic content was obtained from thermal oxidation of dried sediments at 400°C for 12 h. Half of mass-loss was assumed to be organic carbon.
[d]Estimated from organic content data in Fitzgerald (1980).

accompanied the flume in its descent to ensure that it landed properly without undue disturbance to the bed. Then, weights were placed on the flume's feet to ensure that the flume remained stationary during the experiment. The flow rate was stepwise increased at 10-minute intervals; the individual increases were made so that bottom stress increased about 0.1 Pa over 30 s. The turbidity of water passing through the flume was sampled every 15 s with the turbidimeter. The maximum bottom stress applied was 0.5 Pa. Water samples were collected throughout the experiment and later filtered with glass fiber filters (Whatman GFF, Lexington, Mass.) to determine the solids content and thereby calibrate the turbidimeter. The inferred suspended solids concentrations were used in conjunction with the measured flow rates to estimate the erosion rate throughout the experiment. ''Background'' turbidity was measured before and after deployment, but it did not vary significantly.

RESULTS AND DISCUSSION

Field Experiments

Observations of Turbidity Peaks during Flow Accleration

The turbidity/bottom shear stress data from the field indicated that increases in bottom stress always resulted in short-lived peaks in turbidity followed by plateaus (Fig. 4). At sufficiently high stresses (e.g., 0.2 Pa in Fig. 4), the plateaus were clearly above background concentrations indicating that sustained exceedance of the critical shear stress was achieved.

Several possible explanations for the peaks include flow acceleration, flume movement due to flow acceleration, the presence of both easy-to-erode and difficult-to-erode particles, the existence of different modes of erosion (in clumps under high shear versus aggregate by aggregate), and the presence of stress concentration zones (at the entrance and exit of the sediment test section) that were eroded quickly. We believe that the latter explanation has the most currency as scouring was observed within 3 cm of the inlet and exit (in the laboratory), and calculations indicated a correspondence between the amount of scouring observed (i.e., volume of sediment scoured) and the size of the peaks. The postulated stress concentration zones are local nonuniformities in flow. These are in contrast to the larger-scale nonuniformity associated with boundary-layer development in the inlet section. Our analysis (see below) indicated that the overall significance of the peaks was negligible.

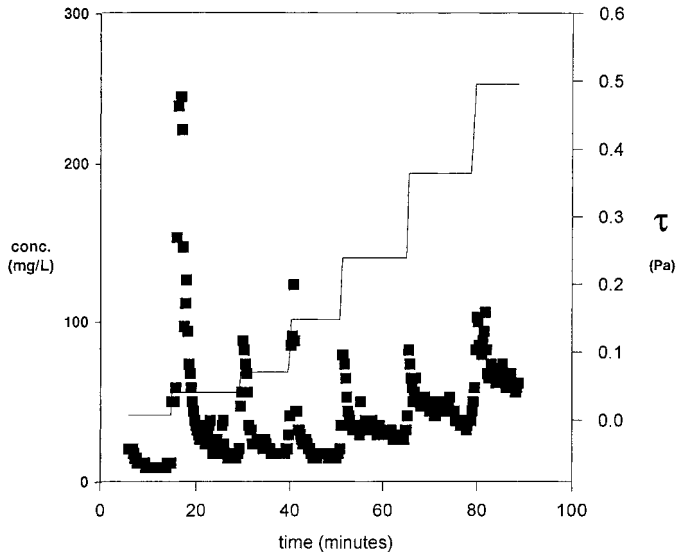

FIG. 4. Suspended Solids Concentration (■, mg/L) and Bottom Stress (——) versus Time during Flume Experiment at Site FL1 on October 19, 1995

Analysis of Turbidity/Flow Rate Data

The turbidity/flow rate time series were analyzed in two ways. First, the rate of erosion occurring in the ''plateaus'' was examined in relation to the inferred bottom stress [Fig. 5(a)]. Analysis of the data assumed an erosional model in which the rate of erosion E (kg m^{-2} s^{-1}) was linearly proportional to the ''excess'' stress τ_{excess} (Pa)

$$E = M\tau_{excess} \tag{3}$$

with

$$\tau_{excess} = \tau - \tau_c \quad \text{for } \tau > \tau_c$$

$$\tau_{excess} = 0 \quad \text{for } \tau < \tau_c$$

where M = erosion rate constant (kg m^{-2} s^{-1} Pa^{-1}) and τ_c = critical shear stress (Pa). Physically, τ_c reflects the average stress required to overcome the gravitational and intraparticle interaction forces holding particles in the bed. The optimal (RMS error minimizing) τ_c and M for this experiment [at FL1 on October 19, Fig. 5(a)] were 0.12 $\pm$ 0.03 Pa and 3.2 $\pm$ 0.2 $\times$ 10^{-3} kg m^{-2} s^{-1} Pa^{-1}, respectively, where the indicated uncertainty reflected the standard error (i.e., deviation) of the parameter estimates (based on a linear regression of the data). The standard (RMS) error of the fit was 6.8 $\times$ 10^{-5} kg m^{-2} s^{-1} (N = 4, R^2 = 0.98). It is noteworthy that some erosion occurred at stresses below the calculated critical stress. Probably, the stochastic nature of turbulence, in which even relatively slow flows have occasional high energy eddies, was in part responsible for this erosion (Lavelle et al. 1984). Also, there is no doubt that the sediment bed presents an areally variable distribution of attractive forces to overcome. When a power law erosion model, $E = \alpha\tau^{\eta}$, which assumes no threshold, was used, a second set of erosion parameters was obtained: α = 2.8 $\pm$ 0.5 $\times$ 10^{-3} kg m^{-2} s^{-1} and η = 1.4 $\pm$ 0.1. The standard error of the power law fit was somewhat greater in this case (1.0 $\times$ 10^{-4} kg m^{-2} s^{-1}).

Using the same raw data (from FL1, October 19), a second estimate of M was obtained by examining the cumulative

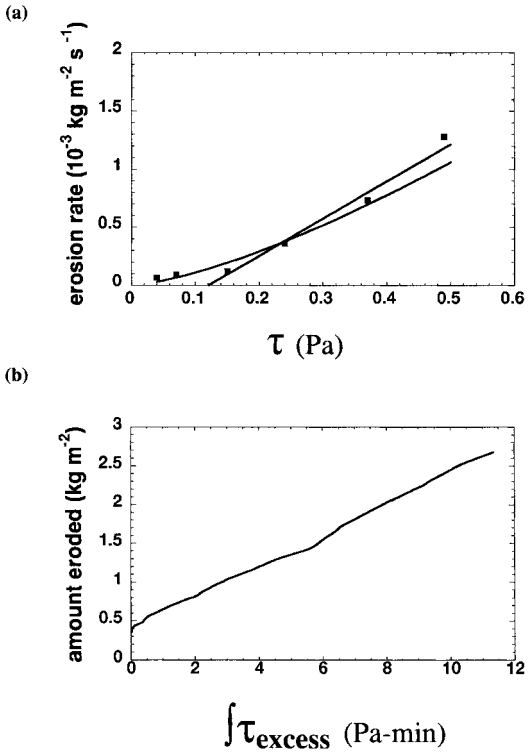

FIG. 5. (a) Erosion Rate versus Bottom Stress τ Based on Plateaus in Concentration Data during Steady Flow Conditions (in Experiment at FL1 on October 19, 1995). Straight Line Represents Best Linear Fit of Data Considering Only Shear Stresses >0.07 Pa: $E = 3.2 \pm 0.3 \times 10^{-3}$ kg m^{-2} s^{-1} Pa^{-1} ($\tau \sim 0.12$ Pa) ($N = 4$, $R^2 = 0.994$). Curved Line Indicates Power Law Fit: $E = 2.8 \times 10^{-3}$ kg m^{-2} s^{-1} $\tau^{-1.4}$. (b) Integral Amount of Sediment Eroded as Function of Time-Integrated Excess Bottom Stress $\int\tau_{excess}$. Slope of Curve Indicates Erosion Rate Constant of $3.4 \pm 0.02 \times 10^{-3}$ kg m^{-2} s^{-1} Pa^{-1}

amount eroded (including the turbidity peaks) as a function of the time-integrated τ_{excess} assuming $\tau_c = 0.12$ Pa [Fig. 5(b)]. The cumulative amount eroded is the time-integration of the observed erosion rate. The linear relationship observed indicated an erosion rate constant (i.e., a slope) of $3.4 \pm 0.02 \times 10^{-3}$ kg cm^{-2} min^{-1} Pa^{-1}. This number is not significantly different from the previously calculated M. Therefore, the presence of the peaks did not have a significant effect on the apparent sediment erodibility in this experiment.

Field Experiment Results

Five additional experiments were conducted at three sites in Quincy Bay during the late summer and early fall of 1995 (Table 2). The first two experiments were conducted before the stabilizing angle irons and weights were added. In these experiments, the peaks that accompanied flow rate increases were relatively large (Fig. 6). The erosion rate constants estimated by the cumulative analysis (including the peaks) were as much as twice as high as the estimates based on the plateaus alone (Fig. 7 and Table 2). It is likely that flume movement during flow acceleration led to spurious erosion and an unrealistically high level of erodibility when the full turbidity time series was analyzed. We believe that the estimates of the erosion parameters, based on the steady flow portion of these experiments (i.e., the plateaus), were most representative of the in situ behaviors. The RMS difference in measured erosion rates between the before-stabilization and after-stabilization experiments (calculated from the linear models) was a maximum of 0.17×10^{-3} kg m^{-2} s^{-1}. This is comparable to the uncertainty (standard error) of the linear erosion model for the October 19 experiment at FL1 (0.15×10^{-3} kg m^{-2} s^{-1}).

The measured erodibilities in four of the experiments—those conducted at sites FL1 and FL2—were fairly invariant (Fig. 8). In one experiment on August 29 at FL1, the τ_c was relatively low (0.04 Pa), but this was compensated for by having a low erosion rate constant. Simultaneously fitting all the data from the four experiments with the ''linear'' erosion model, we obtained $\tau_c = 0.10 \pm 0.04$ Pa and $M = 3.2 \pm 0.2 \times 10^{-3}$ kg m^{-2} s^{-1} Pa^{-1} [$R^2 = 0.92$, $N = 17$, where N is the number of discrete erosion rates measured (one per plateau) in the four experiments]. The standard error of the fit was 1.1×10^{-4} kg m^{-2} s^{-1}. With the power law model, a somewhat better fit was obtained (error = 7.8×10^{-5} kg m^{-2} s^{-1}) with $\alpha = 4.5 \pm 0.8 \times 10^{-3}$ kg m^{-2} s^{-1} and $\eta = 1.7 \pm 0.1$.

The experiments conducted at site FL3 on October 9, 1995, and to some extent on October 26, 1995 (Fig. 8), indicated a significantly reduced sediment erodibility. Divers observed that the sediment during the October 9, 1995 experiment was covered by a greenish-brown film. Microscopic analysis of the surface sediment revealed numerous pennate diatoms. These benthic diatoms were probably from the *Gyrosigma* sp. or *Pleurosigma* sp. (Round et al. 1990). Movement of these diatoms is thought to be mediated by secretions of polysaccharide material. This organic material is left behind by the diatom as it moves, and we speculate that it caused enhanced sedimentary cohesion. During the October 26, 1995 experiment, divers did not observe a diatom film. It is possible that the reduced erodibility measured was due to polysaccharides left behind by the diatoms. During a visit to site FL3 on September 28, 1995 (i.e., before these two experiments were conducted) no algal mats were observed. Thus, such algal influences on sediment erodibility are likely transient (Grant et al. 1986). Also, the fact that no algal mats were observed in a contemporaneous experiment (at site Fl1, October 19) suggests that the mats are spatially limited.

Variation of Erosion Properties with Depth

The issue of variation of sediment erodibility with depth must be considered if the results obtained here are to be useful in sediment transport models. There is certainly potential for significant variation in erosion parameters on a centimeter

TABLE 2. Erosion Parameters Obtained from Quincy Bay Flume Experiments

Flume experiment site (1)	Date of flume experiment (2)	τ_c (Pa) (3)	M, plateau (10^{-3} kg m^{-2} s^{-1} Pa^{-1}) (4)	M, all data (10^{-3} kg m^{-2} s^{-1} Pa^{-1}) (5)
FL1	8/17/95[a]	0.082 ± 0.014	2.8 ± 0.15	6.2 ± 0.03
FL1	8/29/95[a]	0.043 ± 0.020	2.0 ± 0.2	3.2 ± 0.02
FL1	10/19/95	0.12 ± 0.03	3.2 ± 0.3	3.4 ± 0.02
FL2	9/14/95[b]	0.09 ± 0.04	3.7 ± 0.5	4.5 ± 0.03
FL3	10/9/95	0.03 ± 0.08	0.25 ± 0.2	0.27 ± 0.003
FL3	10/26/95	0.035 ± 0.03	1.1 ± 0.01	1.2 ± 0.003

[a]Flume lacked additional stabilizing bars and weights.
[b]Flume was weighted but lacked additional stabilizing bars.

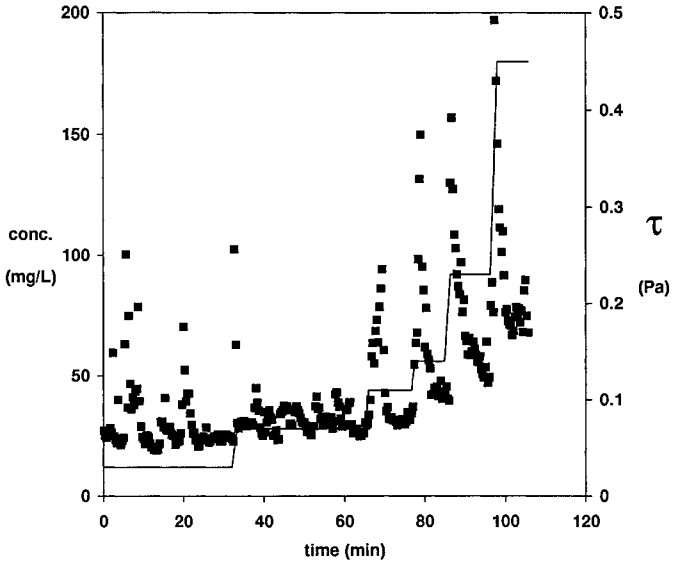

FIG. 6. Suspended Solids Concentration (■, mg/L) and Bottom Stress (——) versus Time during Flume Experiment at Site FL1 on August 17, 1995

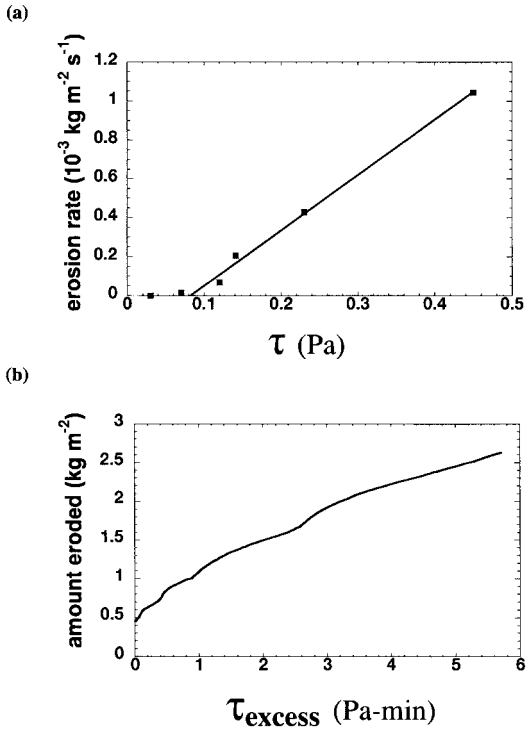

FIG. 7. (a) Erosion Rate versus Bottom Stress τ Based on Plateaus in Turbidity Data during Steady Flow Conditions (in Experiment at FL1 on August 17, 1995). Straight Line Represents Best Linear Fit of Data Considering Only Shear Stresses >0.07 Pa: $E = 2.8 \pm 0.15 \times 10^{-3}$ kg m^{-2} s^{-1} Pa^{-1} ($\tau \sim 0.08$ Pa) ($N = 4$, $R^2 = 0.98$). (b) Integral Amount of Sediment Eroded as Function of Time-Integrated Excess Bottom Stress $\int \tau_{excess}$. Slope of Curve Indicates Erosion Rate Constant of $6.2 \pm 0.03 \times 10^{-3}$ kg m^{-2} s^{-1} Pa^{-1} ($N = 257$, $R^2 = 0.99$)

scale (Zreik et al. 1995; McNeil et al. 1996). For instance, Zreik et al. (1995), using a fall cone device to measure shear strength of surface sediment at a site near Peddocks Island in Boston Harbor, found a 40% increase in shear strength in going from the bed surface to a depth of 30 mm. Assuming a linear relationship between τ_c and sediment depth, the decrease in sediment erodibility for the near-surface sediment (2–3 mm) considered in our work might only amount to a few percent effect.

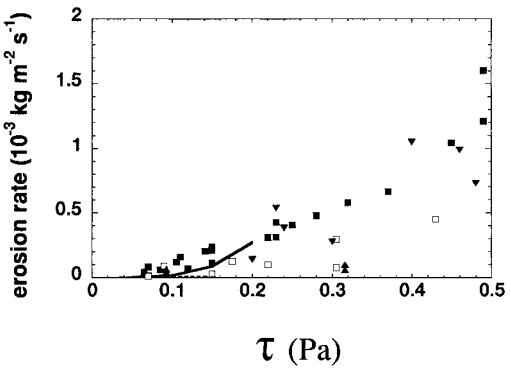

FIG. 8. Comparison of In Situ Measured Erosion Rates from this Study (■, Sites FL1 and FL2; □, Diatom Influenced Site FL3); Chesapeake Bay In Situ Flume Study [▼, Cherrystone Site in Maa and Lee (1997)]; Puget Sound In Situ Flume Study [▲, Stations 1 and 2, Gust and Morris (1989)]; Nearby Puget Sound Study of Tidal Resuspension (——, Lavelle et al. (1984)]; and Chesapeake Bay Study of Tidal Resuspension of Dredged Sediments [– – –, Sanford et al. (1991)]. All Sites Had Silty Sediment or Combination of Fine Sand and Silt in High Salinity Water (>15‰)

Fortunately, analyses of the plateau portions of our experiments (i.e., the observed decrease in turbidity with time under steady flow conditions) provided a basis for estimating the variation of sediment erodibility with depth. Extending the previous work, the erosion rate was analyzed in relation to the bottom stress as well as in relation to the vertical position z (cm) in the sediment. Furthermore, instead of calculating an average erosion rate for the whole plateau, the individual or instantaneous erosion rate ''measurements'' (about 40/plateau) were employed. As before, the linear erosion rate model [(4)] was used

$$E = M(\tau - \tau_c) \tag{4}$$

but here the erosion parameters were allowed to vary linearly with depth (i.e., $\tau_c = \tau_{c,0} + az$; $M = M_0 + bz$). The vertical position during the flume experiment was estimated on the basis of the rate of erosion and the bulk density ($z = \int E\rho_b^{-1} dt$, Table 3). The position was estimated assuming that the sediment in the peaks from local scour and did not relate to the overall removal of the sediment in the test section. Optimization of the fit of (4) to our data led to τ_c (Pa) = (0.093 ± 0.005) + (0.75 ± 0.06 Pa cm^{-1})z and M (kg m^{-2} s^{-1}) = (0.0023 ± 0.0002) + (0.016 ± 0.002 kg m^{-2} s^{-1} cm^{-1})z, where z is in centimeters. The error was obtained by introducing uncertainty in the optimization input variables (E_z) based on the standard error of these estimates (Table 3) and running the optimization procedure Monte Carlo fashion to obtain a large number (100) of independent estimates of $\tau_{c,0}$, M_0, a, and b (Press et al. 1992, p. 690).

The parameters obtained suggest that both the critical shear stress and the erosion rate constant were sensitive to depth (both approximately doubling by $z = 0.1$ cm.). However, these effects largely canceled each other out when their effect on erosion rate is considered. For a range of bottom stresses (0.2–0.5 Pa) and depths (0–0.3 cm) into the sediment, the erosion rates predicted by the depth-varying parameters were compared with the depth-neglecting parameters (Table 4). For the most part, there was reasonably good agreement (within 30%) between the erosion rate estimates based on the two different parameter sets. However, when we were relatively deep into the sediment (0.2–0.3 cm) and at low levels of stress ($\tau < 0.4$ Pa), the depth-neglecting parameters would overestimate erosion rate considerably. Considering the nature of actual resuspension events at these sites in Quincy Bay, this may not be a serious limitation as relatively high stresses ($\tau_{excess} \sim 0.6$ Pa

TABLE 3. Summary of Analysis of Erosion Rate and Depth of Sediment Eroded under Steady Flow Conditions Based on October 19, 1995 Flume Experiment at FL1 (Fig. 4)

Data (1)	τ = 0.15 Pa; Q = 1.7 L s^{-1} (2)	τ = 0.24 Pa; Q = 2.2 L s^{-1} (3)	τ = 0.37 Pa; Q = 2.8 L s^{-1} (4)	τ = 0.49 Pa; Q = 3.2 L s^{-1} (5)
Range of time covered in analysis (min)[a]	42.5–50.75	54–64	68–75[b]	82.3–88.8
$C_{average}$ (mg/L)[c]	10.5 ± 3.6	23 ± 5	38 ± 3	58 ± 5
E (10^{-3} kg m^{-2} s^{-1})[c,d]	0.12 ± 0.04	0.35 ± 0.05	0.73 ± 0.05	1.28 ± 0.09
$\Delta z_{analyzed}$[c,e] (cm)	0.010	0.036	0.051	0.083
Total extent of time at particular stress (min)[a]	40.25–50.5	51–65	65.5–79	79.5–88.8
Δz_{total} at particular stress (cm)[f]	0.012	0.050	0.098	0.118
Depths eroded at particular stress (cm)	0.01[g]–0.022	0.022–0.072	0.072–0.17	0.17–0.29

[a]Times refer to those in Fig. 4.
[b]End time of second plateau was chosen before dip in sediment concentration (Fig. 4), which was probably derived from poorly controlled flow rate.
[c]During analyzed time.
[d]E is average erosion rate calculated as $C_{average}Q/A$, where $C_{average}$ is the average sediment concentration during analyzed time (Fig. 4) and A is test area = 0.155 m^2.
[e]$\Delta z_{analyzed}$ is estimated as $E\Delta t_{analyzed}\rho_b^{-1}$, where $\Delta t_{analyzed}$ is amount of time analyzed and is sediment bulk density calculated as [(1 − porosity) · 2.5 g/mL].
[f]Δz_{total} is $(\Delta t_{total}/\Delta t_{analyzed})\Delta z_{analyzed}$, where Δt_{total} is total time at particular stress.
[g]Amount of prior erosion assuming sediment in peaks is coming only from scour zones.

TABLE 4. Erosion Rates (10^{-3} kg m^{-2} s^{-1}) as Function of Bottom Stress τ and Depth into Sediment z on Basis of Erosion Parameters (τ_c and M) Deduced Neglecting Depth Dependencies and Depth-Dependent Parameters [$\tau_c(z)$ and $M(z)$]

	Erosion Rate from Parameters Neglecting Depth Variation	Erosion Rate from Parameters with Depth Dependency			
τ (Pa) (1)	τ_c = 0.12 Pa; M = 3.2 g m^{-2} s^{-1} (z independent) (2)	$\tau_c(z)$ = 0.093 Pa; $M(z)$ = 2.3 g m^{-2} s^{-1} (z = 0) (3)	$\tau_c(z)$ = 0.17 Pa; $M(z)$ = 3.9 g m^{-2} s^{-1} (z = 0.1 cm) (4)	$\tau_c(z)$ = 0.24 Pa; $M(z)$ = 5.4 g m^{-2} s^{-1} (z = 0.2 cm) (5)	$\tau_c(z)$ = 0.32 Pa; $M(z)$ = 7.0 g m^{-2} s^{-1} (z = 0.3 cm) (6)
0.2	0.26	0.25	0.12	0	0
0.3	0.58	0.48	0.51	0.32	0
0.4	0.90	0.71	0.90	0.86	0.56
0.5	1.2	0.94	1.29	1.4	1.26

or $\tau \sim 0.7$ Pa) would be necessary to erode 0.2 cm of sediment in the first place (Ravens 1997). The latter result follows from the relatively weak current and eddy diffusivity at these sites and from the relatively fast settling velocity of particles [3 m/h (Ravens 1997)]. Thus, the depth-neglecting parameters appear to work reasonably well at these sites. However, one should be cautioned against using these parameters in an application in which significantly greater than 0.3 cm of sediment was eroded or where the hydrodynamic and sediment conditions differed significantly from the Quincy Bay sites.

Comparison with Other In Situ Erosion Measurements

The critical shear stress estimate from these erosion experiments (0.10 ± 0.04 Pa) is consistent with a deduced τ_c value of 0.085 Pa based on the correlation of sand content and time-integrated excess stress in Quincy Bay (Ravens et al. 1998). In addition, the estimate is in general agreement with other in situ experiment-based estimates from other high salinity (>15‰) estuaries with consolidated silty or silty and sandy sediment. For example, Young (1975), working in Buzzards Bay in southeastern Massachusetts, reported an in situ critical shear stress of 0.08 Pa. Maa and Lee (1997), working in lower Chesapeake Bay, reported critical shear stresses ranging from 0.11 to 0.14 Pa. Somewhat anomalously, Sanford et al. (1991), working in northern Chesapeake Bay at a disposal site for dredged sediments, reported a critical shear stress of only 0.02 Pa. However, this was probably an indication of the erodibility of unconsolidated ''fluff.'' Maa and Lee (1997) reported about the same critical stress for fluff.

The measured erosion rates reported here are also in reasonable agreement with other in situ measurements of consolidated silty or silty and sandy sediments in high salinity (>15‰) estuaries (Fig. 8). The measured erosion rates shown were based on both flume measurements, as well as analysis of natural resuspension events. In addition to the algal-mat-influenced data from this study, only the flume results in Puget Sound [solid triangle in Fig. 8, Gust and Morris (1989)] and the tidal resuspension results of Sanford et al. (1991) appear to be out of character. It is noteworthy that the reported Puget Sound flume results are also not consistent with erosion rate estimates based on analysis of tidal current-derived resuspension at nearby sites (Lavelle et al. 1984). Perhaps, this is due to heterogeneity at the Puget Sound site.

The lack of variability in erodibility is somewhat surprising because the range of some of the environmental parameters (e.g., organic carbon content from 0.5% in Chesapeake Bay to 5% in Puget Sound) should have translated to quite a different erodibility according to some laboratory studies (Young 1975). Perhaps the relatively uniform erodibility of natural sediments is related to the agitation they all receive from benthic infauna. Most of the laboratory experiments that demonstrate the relevance of various environmental parameters were performed in the absence of biological influences. Thus, the ''leveling'' effect of biological processes may not be evident in the laboratory experiments.

CONCLUSIONS

We used a ''straight'' flume in situ to measure the erodibility of cohesive sediments in Boston Harbor using a trip bar to enhance boundary-layer development and a roughened false bottom to limit premature scouring. Except in the presence of an algal mat, erodibility in Quincy Bay was quite consistent, exhibiting a τ_c near 0.1 Pa and an erosion rate near 3×10^{-3} kg m^{-2} s^{-1} Pa^{-1}. The algal mats led to an order of magnitude

decrease in sediment erodibility. In the absence of algal mats, the observed erodibility was very similar to that seen in other in situ studies of high salinity, silty (or silty and sandy) sediments. Depth-dependent erodibility parameters were also calculated. Both the critical shear stress and erosion rate constant were found to increase with depth (approximately doubling by 1 mm in the sediment).

ACKNOWLEDGMENTS

This work was funded by the Office of Naval Research (Grant No. NOOO14-94-1-0752). The Massachusetts Institute of Technology Sailing Pavillion lent boats. Numerous people helped with the field and laboratory work including David Shull, Christine Hartman, Pardo Ignaciez, Lukas Wick, Hank Seaman, Rene Kim, Chris Swartz, Louke Ellenbroek, Analia Barrantes de Karma, and John MacFarlane. Ole Madsen and Eric Adams provided valuable feedback and advice.

APPENDIX I. REFERENCES

Butman, C. A., and Chapman, R. J. (1989). ''The 17-meter flume at the Coastal Research Laboratory. Part 1: Description and user's manual.'' *Tech. Rep. 89-10*, Woods Hole Oceanographic Institution, Woods Hole, Mass.

Daborn, G. R., et al. (1993). ''An ecological cascade effect: Migratory birds affect stability of intertidal sediments.'' *Limnol. Oceanogr.*, 38(1), 225–231.

Daily, J. W., and Harleman, D. R. F. (1966). *Fluid dynamics*. Addison-Wesley, Reading, Mass.

Fitzgerald, M. (1980). ''Anthropogenic influence of the sedimentary regime on an urban estuary, Boston Harbor,'' PhD dissertation. Woods Hole Oceanographic Institution, Woods Hole, Mass.

Gardner, G. R., and Pruell, R. J. (1988). *A histopathological and chemical assessment of winter flounder, lobster, and soft-shelled clam indigenous to Quincy Bay, Boston Harbor and an in situ evaluation of oysters including sediment (surface and cores) chemistry*. USEPA ERL. Narragansett, R.I.

Graf, W. H. (1984). *Hydraulics of sediment transport*. McGraw-Hill, New York.

Grant, J., Bathmann, U. V., and Mills, E. L. (1986). ''The interaction between benthic diatom films and sediment transport.'' *Estuarine Coast. Shelf Sci.*, 23, 225–238.

Gust, G., and Morris, M. J. (1989). ''Erosion thresholds and entrainment rates of undisturbed in-situ sediments.'' *J. Coast. Res.*, 5, 87–99.

Holland, A. F., Zingmark, R. B., and Dean, J. M. (1974). ''Quantitative evidence concerning the stabilization of sediment by benthic diatoms.'' *Marine Biol.*, 27, 191–196.

Krone, R. B. (1976). ''Engineering interest in the benthic boundary layer.'' *The benthic boundary layer*, I. N. McCave, ed., Plenum, New York, 143–156.

Lavelle, J. W., Mofjeld, H. O., and Baker, E. T. (1984). ''An in situ erosion rate for a fine-grained marine sediment.'' *J. Geophys. Res.*, 89(C4), 6543–6552.

Leo, W. S., Connor, M. S., Keay, K., and Rex, A. (1993). ''Contaminated sediments in Boston Harbor.'' *Rep. No. 93-9*, Massachusetts Water Resources Authority, Boston, Mass.

Luettich, R. A., Harleman, D. R. F., and Somlyody, L. (1990). ''Dynamic behavior of suspended sediment concentrations in a shallow lake perturbed by episodic wind events.'' *Limnol. Oceanogr.*, 35(5), 1050–1067.

Maa, J. P.-Y. (1993). ''VIMS sea carousel: Its hydrodynamic characteristics.'' *Nearshore and estuarine cohesive sediment transport (Coastal and estuarine studies, 42)*, A. J. Mehta, ed., American Geophysical Union, Washington, D.C., 265–280.

Maa, J. P.-Y., and Lee, C.-H. (1997). ''Variation of the resuspension coefficients in the lower Chesapeake Bay.'' *J. Coast. Res.*, 25, 63–74.

Maa, J. P.-Y., Wright, L. D., Lee, C.-H., and Shannon, T. W. (1993). ''VIMS sea carousel: A field instrument for studying sediment transport.'' *Marine Geol.*, 115, 271–287.

McCave, I. N. (1984). ''Erosion, transport, and deposition of fine-grained marine sediments.'' *Fine-grained sediments: Deep-water processes and facies*, D. A. V. Stow and D. J. W. Piper, eds., Blackwell Scientific, Oxford, England, 35–69.

McNeil, J., Taylor, C., and Lick, W. J. (1996). ''Measurement of erosion of undisturbed bottom sediments with depth.'' *J. Hydr. Engrg.*, ASCE, 122(6), 316–324.

Press, W. H., Teukolsky, S. A., Vetterling, W. T., and Flannery, B. P. (1992). *Numerical Recipes in C*, 2nd Ed., Cambridge University Press, New York.

Ravens, T. M. (1997). ''Sediment resuspension in Boston Harbor,'' PhD dissertation, Massachusetts Institute of Technology, Cambridge, Mass.

Ravens, T. M., Madsen, O. S., Signell, R. P., Adams, C. E., and Gschwend, P. M. (1998). ''Hydrodynamic forcing and sediment character in Boston Harbor.'' *J. Wtrwy., Port, Coast., Oc. Engrg.*, ASCE, 124(1), 40–42.

Rhoads, D. C., Yingst, J. Y., and Ullman, W. (1978). ''Sea floor stability in central Long Island Sound: Part I. Temporal changes in erodibility of fine-grained sediment.'' *Estuarine interactions*, M. L. Wiley, ed., Academic, New York, 221–224.

Round, F. E., Crawford, R. M., and Mann, D. G. (1990). *The diatoms: Biology & morphology of the genera*. Cambridge University Press, Cambridge, England.

Sanford, L. P., Panageotou, W., and Halka, J. P. (1991). ''Tidal resuspension of sediments in northern Chesapeake Bay.'' *Marine Geol.*, 97, 87–103.

Shiaris, M. P., and Jambard-Sweet, D. (1986). ''Baseline polycyclic aromatic hydrocarbons in surficial sediments of Boston Harbor, Massachusetts, USA.'' *Marine Pollution Bull.*, 17(10), 469–472.

Signell, R. P., and Butman, B. (1992). ''Modeling tidal exchange and dispersion in Boston Harbor.'' *J. Geophys. Res.*, 97(C10), 15,591–15,606.

Young, R. A. (1975). ''Flow and sediment properties influencing erosion of fine-grained marine sediments: Sea floor and laboratory experiments,'' PhD dissertation, Woods Hole Oceanographic Institution, Woods Hole, Mass.

Zreik, D. A., Ladd, C. C., and Germaine, J. J. (1995). ''A new fall cone device for measuring the undrained strength of very weak cohesive soils.'' *Geotech. Testing J.*, 18, 472–482.

APPENDIX II. NOTATION

The following symbols are used in this paper:

E = erosion rate (kg m^{-2} s^{-1});
f = friction factor (dimensionless);
M = erosion rate constant (kg m^{-2} s^{-1} Pa^{-1});
Q = flow rate (L s^{-1});
U = cross-sectional area-averaged velocity (m s^{-1});
z = vertical position (origin at sediment-water interface and positive downward) (cm);
α = pre-exponential factor in erosion rate power law (MKS units);
η = exponent in erosion rate power law (SI units);
ρ = water density (kg m^{-3});
τ = bottom shear stress (Pa);
τ_c = critical shear stress (Pa); and
τ_{excess} = excess bottom shear stress (Pa).